JPE 13-6-4

http://dx.doi.org/10.6113/JPE.2013.13.6.955
ISSN(Print): 1598-2092 / ISSN(Online): 2093-4718

A Time-Varying Gain Super-Twisting Algorithm to Drive a SPIM

Noureddaher Zaidi[†], Mohamed Jemli[*], Hechmi Ben Azza[*], and Mohamed Boussak[**]

[†*]C3S Research Unit, High School of Science and Techniques of Tunis, University of Tunis, Tunisia
[**]LSIS, CNRS UMR 6168, Centrale Marseille Recherche et Technologies, Ecole Centrale Marseille, France

Abstract

To acquire a performed and practical solution that is free from chattering, this study proposes the use of an adaptive super-twisting algorithm to drive a single-phase induction motor. Partial feedback linearization is applied before using a super-twisting algorithm to control the speed and stator currents. The load torque is considered an unknown but bounded disturbance. Therefore, a time-varying switching gain that does not require prior knowledge of the disturbance boundary is proposed. A simple sliding surface is formulated as the difference between the real and desired trajectories obtained from the indirect rotor flux oriented control strategy. To illustrate the effectiveness of the proposed control structure, an experimental setup around a digital signal processor (dS1104) is developed and several tests are performed.

Keywords: Adaptive Super-Twisting Algorithm, Chattering, DSP implementation, Single-Phase Induction Motor, Sliding Mode Control, Vector Control

I. INTRODUCTION

Single-phase induction motors (SPIMs) have long been used in several domestic and industrial applications that require low-power motors operating at a fixed speed. In this operating mode, the developed electromagnetic torque presents a pulsating behavior, thus negatively affecting the performances of motors and reducing their use. Motivated by the cost significantly reduction, variable-speed drives have recently been integrated into such applications. This integration aims to improve the SPIM performances, saves a considerable amount of energy and enhances induction motor efficiency [1]–[4]. Thus, variable-speed SPIM drives have continued to attract the attention of industrial and scientific communities.

Various controller structures to drive SPIMs have been encountered in contemporary literature. In [5]–[7], linear proportional integral controllers are included in the field oriented control schema to drive a SPIM. In [8], two synchronous controllers are used: the positive-sequence synchronous controller intended to annul the direct sequence term and the negative-sequence synchronous controller intended to annul the inverse-sequence term. A diametrical inversion of the stator voltages is adopted in [9]. All previous controller structures suffer from non-neglected currents and torque oscillations or loss of robustness against parameter variations at low speed ranges.

The sliding mode technique has been investigated to drive SPIMs speed in [10]–[12]. In [11], some extra blocks are needed to estimate the rotor flux and load torque. Thus, this control schema is not always suitable for real-time implementation.

Nevertheless, the sliding mode control technique is still a promising technique for designing control schemas thanks to several significant advantages, namely, fast response, invariance against uncertainty conditions, and simple implementation [13]–[15]. In any conventional sliding mode control implementation, the chattering phenomenon must be considered to prevent dangerous high-frequency vibrations and actuator damage [16], [17]. The chattering phenomenon causes high oscillation in the proximity of the sliding surface (SS). Thus, various approaches have been extensively studied to reduce the effects of chattering. These approaches can be classified into two categories according to the nature of the switching gain. The first category involves low-pass filtering, the boundary layer, and high-order sliding mode techniques with a fixed switching gain [18]–[21]. In most cases, this gain

Manuscript received Mar. 19, 2013; revised Jul. 25, 2013
Recommended for publication by Associate Editor Sanjeet K. Dwivedi.
Corresponding Author: zaidi.nour@unite-c3s.com
Tel: +216-97-226-760, Fax: +216-73-369-506, University of Tunis
[*]C3S Research Unit, High School of Science and Techniques of Tunis, University of Tunis, Tunisia
[**]LSIS, CNRS UMR 6168, Centrale Marseille Recherche et Technologies, Ecole Centrale Marseille, France

is overestimated or is fixed great for time convergence reasons even though the high-order sliding technique may lose its chattering elimination ability. Moreover, all cited approaches require prior knowledge of the upper bound of external disturbances or parameter uncertainties to determine the switching gain. However, in many applications, these boundaries are not always known or at least difficult to find, as in our case. To overcome this problem, research communities are oriented to the second category of approaches based on the concept of adaptive sliding mode gain. A supplementary amelioration with respect to time convergence and chattering elimination is then registered. These approaches include the time-varying gain and state-depending gain methods [22]–[27].

In this study, we propose a novel indirect rotor flux oriented control (IRFOC) strategy to drive the SPIM speed. The controllers' synthesis is based on an adaptive super-twisting algorithm (ASTA). The adopted time-varying control law tries to improve previous controllers by eliminating or reducing torque oscillations. The time-varying switching gain aims to improve the chattering suppression capability required for practical implementation. The design of the ASTA requires partial feedback linearization before being used to drive the SPIM. The ASTA also operates without the need for prior knowledge of upper-limit disturbances.

The paper is organized as follows. The dynamic SPIM model and IRFOC strategy are presented in Section 2. Section 3 discusses the design of the proposed speed and current controllers based on ASTA. Section 4 presents and evaluates the developed laboratory setup and experimental results.

II. SPIM SYMMETRIC MODEL AND IRFOC STRATEGY

The input–output SPIM state space model in a stationary reference frame can be expressed as follows:

$$\frac{d}{dt}X = AX + BU \ , \tag{1}$$

where:

- $X = \left[i_{s\alpha} \quad i_{s\beta} \quad \varphi_{r\alpha} \quad \varphi_{r\beta} \quad \omega \right]^T$, $U = \left[v_{s\alpha} \quad v_{s\beta} \quad T_l \right]^T$;
- $v_{s\alpha}$, $v_{s\beta}$ / $i_{s\alpha}$, $i_{s\beta}$: stator voltages/currents in a stationary reference frame;
- $\varphi_{r\alpha}$, $\varphi_{r\beta}$: rotor fluxes in a stationary reference frame;
- ω: rotor angular frequency;
- T_l: load torque.

Matrices A and B are expressed as follows:

$$A = \begin{bmatrix} -\frac{1}{\sigma_{sd}\tau_{sd}} - \frac{1-\sigma_{sd}}{\sigma_{sd}\tau_r} & 0 & \frac{1-\sigma_{sd}}{\sigma_{sd}\tau_r M_{srd}} & \frac{1-\sigma_{sd}}{\sigma_{sd} M_{srd}}\omega & 0 \\ 0 & -\frac{1}{\sigma_{sq}\tau_{sq}} - \frac{1-\sigma_{sq}}{\sigma_{sq}\tau_r} & \frac{1-\sigma_{sq}}{\sigma_{sq} M_{srq}}\omega & \frac{1-\sigma_{sq}}{\sigma_{sq}\tau_r M_{srq}} & 0 \\ \frac{M_{srd}}{\tau_r} & 0 & -\frac{1}{\tau_r} & -\omega & 0 \\ 0 & \frac{M_{srq}}{\tau_r} & \omega & -\frac{1}{\tau_r} & 0 \\ -n_p^2 \frac{M_{srd}}{JL_r}\varphi_{r\beta} & n_p^2 \frac{M_{srq}}{JL_r}\varphi_{r\alpha} & 0 & 0 & -\frac{f}{J} \end{bmatrix},$$

$$B = \begin{bmatrix} \frac{1}{\sigma_{sd} L_{sd}} & 0 & 0 \\ 0 & \frac{1}{\sigma_{sq} L_{sq}} & 0 \\ 0 & 0 & 0 \\ 0 & 0 & 0 \\ 0 & 0 & -\frac{n_p}{J} \end{bmatrix}.$$

where:

$$\tau_{sd} = \frac{L_{sd}}{R_{sd}}, \tau_{sq} = \frac{L_{sq}}{R_{sq}}, \ \tau_r = \frac{L_r}{R_r}, \sigma_{sd} = 1 - \frac{M_{srd}^2}{L_{sd} L_r}, \ \sigma_{sq} = 1 - \frac{M_{srq}^2}{L_{sq} L_r};$$

- L_{sd}, L_{sq}, L_r, M_{srd}, M_{srq}: self and mutual inductances of the stator and rotor;
- R_{sd}, R_{sq}, and R_r: resistances of the stator and rotor;
- f and J: friction coefficient and total inertia, respectively;
- n_p: pole pairs number.

The vector control of the induction motor approach achieves a decoupled flux and torque, thus leading to DC motor behavior. This approach can be implemented in many different ways with respect to the chosen oriented flux vector. The IRFOC strategy is commonly used because of its simple implementation. Nevertheless, a direct rotor field orientation technique can be found in [28].

Fig. 1 shows a block diagram of the proposed IRFOC strategy. In addition to the direct current reference and slip frequency block determination, the IRFOC strategy involves three high-order sliding mode controllers. Two of these controllers are intended to control the main and auxiliary winding currents, whereas the third controller drives the SPIM speed. According to this strategy, the outputs of the sliding mode current controllers provide the stator voltage vector, whereas the speed controller generates the electromagnetic torque reference. Tow transformation blocks are required; the first block performs the coordinate transformation from the reference frame aligned along with the rotor flux vector to the stationary reference frame, whereas the second block performs the inverse - coordinate transformation. The main winding is different from the auxiliary winding. Thus, the above model is asymmetric and vector control techniques cannot be directly applied. A symmetric model can be established by using a suitable variable transformation such us in [1, 5] to transform the stator variables.

$$\begin{bmatrix} i_{s\alpha} \\ i_{s\beta} \end{bmatrix} = T \begin{bmatrix} i_{s\alpha 1} \\ i_{s\beta 1} \end{bmatrix}; \begin{bmatrix} v_{s\alpha} \\ v_{s\beta} \end{bmatrix} = T^{-1} \begin{bmatrix} v_{s\alpha 1} \\ v_{s\beta 1} \end{bmatrix} \text{ and } \begin{bmatrix} \varphi_{s\alpha} \\ \varphi_{s\beta} \end{bmatrix} = T^{-1} \begin{bmatrix} \varphi_{s\alpha 1} \\ \varphi_{s\beta 1} \end{bmatrix} \tag{2}$$

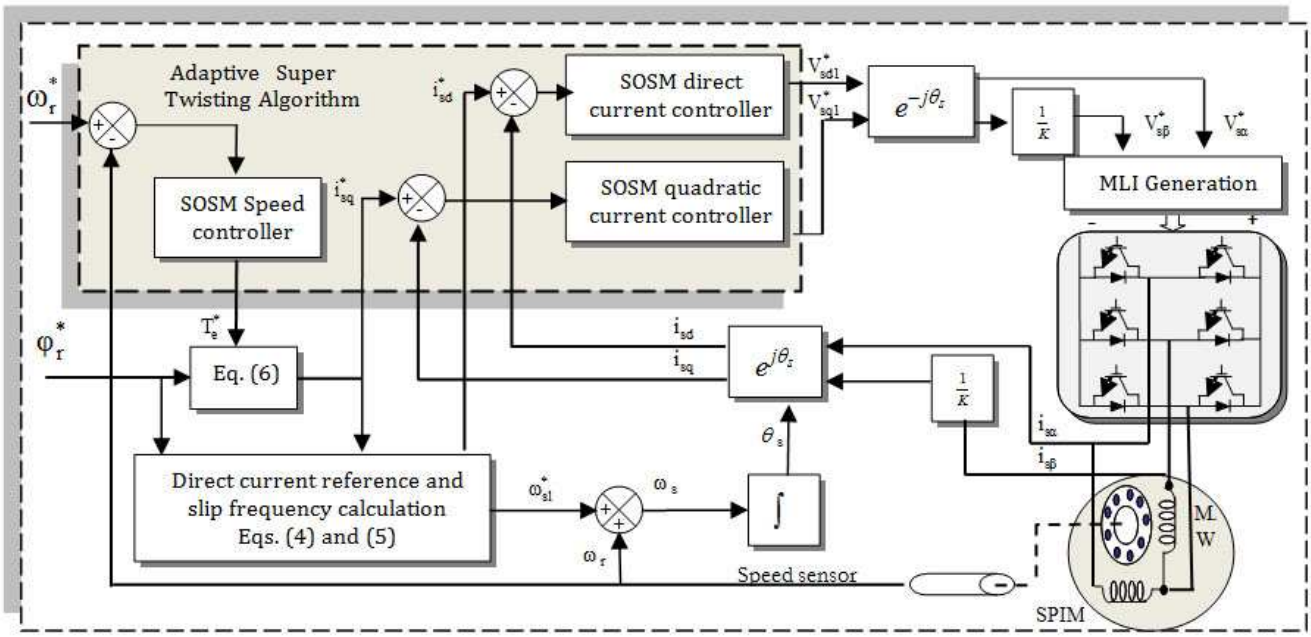

Fig. 1. Block diagram of the proposed IRFOC strategy.

with $T = \begin{bmatrix} 1 & 0 \\ 0 & K \end{bmatrix}$; $K = \frac{M_{srd}}{M_{srq}}$.

The implementation of the IRFOC strategy necessitates the determination of certain reference variables from the flux and electromagnetic torque expressions.

By using the synchronous transformation T_s, the first derivative rotor flux form in a synchronous reference frame (denoted by the superscript d and q) can be obtained as follows:

$$\begin{bmatrix} \dot{\varphi}_{rd} \\ \dot{\varphi}_{rq} \end{bmatrix} = \begin{bmatrix} -\frac{1}{T_r} & \omega_{sl} \\ -\omega_{sl} & -\frac{1}{T_r} \end{bmatrix} \begin{bmatrix} \varphi_{rd} \\ \varphi_{rq} \end{bmatrix} + \begin{bmatrix} \frac{M_{srd}}{T_r} & 0 \\ 0 & \frac{M_{srd}}{T_r} \end{bmatrix} \begin{bmatrix} i_{sd1} \\ i_{sq1} \end{bmatrix}, \tag{3}$$

where: $\begin{bmatrix} \varphi_{rd} \\ \varphi_{rq} \end{bmatrix} = T_s \begin{bmatrix} \varphi_{r\alpha} \\ \varphi_{r\beta} \end{bmatrix}$, $\begin{bmatrix} i_{sd1} \\ i_{sq1} \end{bmatrix} = T_s \begin{bmatrix} i_{s\alpha1} \\ i_{s\beta1} \end{bmatrix}$, $T_s = e^{j\theta_s}$, $\omega_{sl} = \omega_s - \omega_r$.

where T_r represents the rotor constant time.

Given that the d-axis of the reference frame is oriented along the rotor flux vector, we can obtain the requested direct and quadratic current references i_{sd}^*, i_{sq}^*, and the slip frequency ω_{sl}^* expressions.

$$\frac{d}{dt}\varphi_r^* = -\frac{1}{T_r}\varphi_r^* + \frac{M_{srd}}{T_r} i_{sd1}^*, \tag{4}$$

$$\omega_{sl}^* = \frac{M_{srd}}{T_r \varphi_r^*} i_{sq1}^*, \tag{5}$$

$$T_e^* = n_p \frac{M_{srd}}{L_r} \varphi_r^* i_{sq1}^*. \tag{6}$$

III. Adaptive Super-Twisting Controllers Design

The conventional sliding mode controller and second-order sliding mode (SOSM) controllers, including continuous super-twisting algorithm (STA), can elaborate a robust control law if the boundaries of the uncertainties or disturbances are known a priori. Have a good knowledge of boundaries represent a severe constraint for many practical cases, such as in SPIM. The aim of this study is to elaborate an adaptive STA gain to drive the SPIM speed. The control gains are continuously adapted to cancel finite unknown disturbances, and the ability to generate a control signal that is free of chattering must be preserved.

A. Problem Formulation

Assuming that the load torque is considered an unknown external perturbation, knowing that the rotor flux is oriented along the d-axe, and considering the above transformation, we can establish the expressions of the main and auxiliary winding currents and the speed in a synchronous reference as follows:

$$\frac{d}{dt}\begin{bmatrix} i_{sd1} \\ i_{sq1} \\ \omega \end{bmatrix} = -\frac{1}{L_{sd}\sigma_{sd}} \left(\begin{bmatrix} (R_{sd} + \frac{M_{srd}^2}{T_r L_r}) & \omega_s & 0 \\ -\omega_s & (K^2 R_{sq} + \frac{M_{srd}^2}{T_r L_r}) & 0 \\ 0 & 0 & L_{sd}\sigma_{sd}\frac{f}{J} \end{bmatrix} \begin{bmatrix} i_{ds1} \\ i_{qs1} \\ \omega \end{bmatrix} + \begin{bmatrix} v_{sd1} + \frac{M_{srd}}{T_r L_r}\varphi_r \\ v_{sq1} - \frac{M_{srd}}{L_r}\omega\varphi_r \\ L_{sd}\sigma_{sd}\frac{n_p}{J}T_e \end{bmatrix} \right), \tag{7}$$

Adopting the following partial feedback linearization:

$$\begin{bmatrix} U_d \\ U_q \\ U_\omega \end{bmatrix} = \begin{bmatrix} v_{sd1} + \dfrac{M_{srd}}{T_r L_r}\varphi_r \\ v_{sq1} - \dfrac{M_{srd}}{L_r}\omega\varphi_r \\ L_{sd}\sigma_{sd}\dfrac{n_p}{J}T_e \end{bmatrix}. \quad (8)$$

Equation (7) becomes the following:

$$\frac{d}{dt}\begin{bmatrix} i_{sd1} \\ i_{sq1} \\ \omega \end{bmatrix} = -\frac{1}{L_{sd}\sigma_{sd}}\left(\begin{bmatrix} (R_{sd} + \dfrac{M_{srd}^2}{T_r L_r}) & \omega_s & 0 \\ -\omega_s & (K^2 R_{sq} + \dfrac{M_{srd}^2}{T_r L_r}) & 0 \\ 0 & 0 & L_{sd}\sigma_{sd}\dfrac{f}{J} \end{bmatrix}\begin{bmatrix} i_{sd1} \\ i_{sq1} \\ \omega \end{bmatrix} + \begin{bmatrix} U_d \\ U_q \\ U_\omega \end{bmatrix}\right). \quad (9)$$

Considering the following error expression:

$$\begin{bmatrix} \varepsilon_{sd} \\ \varepsilon_{sq} \\ \varepsilon_\omega \end{bmatrix} = \begin{bmatrix} i_{sd1} - i_{sd1}^* \\ i_{sq1} - i_{sq1}^* \\ \omega - \omega^* \end{bmatrix}. \quad (10)$$

where * denotes the reference variables, and i_{sd1} and i_{sq1} represent the transformed measured stator currents expressed in a synchronously rotating reference frame.

The stator currents references are obtained from Equations (5) and (6) (Fig. 1). The SSs can be defined based on the stator currents and rotor speed errors:

$$\begin{bmatrix} S_d \\ S_q \\ S_\omega \end{bmatrix} = \begin{bmatrix} c_d \\ c_q \\ c_\omega \end{bmatrix}\begin{bmatrix} \varepsilon_{sd} \\ \varepsilon_{sq} \\ \varepsilon_\omega \end{bmatrix}; \quad c_d, c_q \text{ and } c_\omega \succ 0. \quad (11)$$

By substituting the reference terms in Equation (9), the first derivative forms of the errors are as follows:

$$\frac{d}{dt}\begin{bmatrix} \varepsilon_d \\ \varepsilon_q \\ \varepsilon_\omega \end{bmatrix} = -\frac{1}{L_{sd}\sigma_{sd}}\left(\begin{bmatrix} (R_{sd} + \dfrac{M_{srd}^2}{T_r L_r}) & \omega_s & 0 \\ -\omega_s & (K^2 R_{sq} + \dfrac{M_{srd}^2}{T_r L_r}) & 0 \\ 0 & 0 & L_{sd}\sigma_{sd}\dfrac{f}{J} \end{bmatrix}\begin{bmatrix} \varepsilon_d \\ \varepsilon_q \\ \varepsilon_\omega \end{bmatrix} + \begin{bmatrix} \Delta U_d \\ \Delta U_q \\ \Delta U_\omega \end{bmatrix}\right), \quad (12)$$

where: $\begin{bmatrix} \Delta U_d \\ \Delta U_q \\ \Delta U_\omega \end{bmatrix} = \begin{bmatrix} U_d - U_d^* \\ U_q - U_q^* \\ U_\omega - U_\omega^* \end{bmatrix}$.

However, since the dynamics of the electrical variables are faster than the dynamics of the mechanical variables, the feedback linearization terms can be considered constants. Thus, the control variation terms may be expressed as follows:

$$\begin{bmatrix} \Delta U_d \\ \Delta U_q \\ \Delta U_\omega \end{bmatrix} = \begin{bmatrix} v_{sd1} - v_{sd1}^* \\ v_{sq1} - v_{sq1}^* \\ U_\omega - U_\omega^* \end{bmatrix}. \quad (13)$$

The vector ΔU is considered the control law variation required to force the state variables to reach the SSs. Thus, the error dynamics can be presented in a compact form as follows:

$$\frac{d}{dt}\varepsilon = \phi(x,t) + \varpi, \qquad \varpi = b(x,t)\Delta U, \quad \text{where} \quad b(x,t) = -\frac{1}{L_{sd}\sigma_{sd}}. \quad (14)$$

B. STA Control Law With Time-Varying Gain Design

The solution of Eq. (14) is understood in the sense of Filippov [25]. The function b(x, t) is considered bounded and ≠ 0 for all times, where x represents the state vector. Assume the following:

$$\left|\phi(x,t)\right| \le \delta\left|S\right|^{\frac{1}{2}}. \quad (15)$$

where δ > 0 exists but is not known.

The main objective is to drive the selected SS and its derivative within to zero in a finite time in the presence of bounded uncertainties and disturbances without knowing the upper-limit value. The STA is one of the most powerful SOSM controllers and has been proposed to control systems with a relative degree 1. This algorithm ensures that the states can slide on the chosen SS, that is, S, by using only the measurement of S. The control law consists of two terms that are formulated around the sliding variables [20, 21]. The first term is the integral of a discontinued function, whereas the second term represents a continuous function to alleviate the chattering effect. The classical STA control law expression is as follows:

$$\begin{cases} \varpi = u_1 - \alpha\left|\varepsilon_{sd1}\right|^\rho \text{Sign}(S) \\ \dfrac{d}{dt}u_1 = -\beta\text{Sign}(S) \end{cases}, \quad (16)$$

where ρ, α, and β represent the tuning controller parameters, which are positive constants.

Consider the following adaptive control gains α and β:

$$\begin{cases} \alpha = \alpha(S, \dot{S}, t) \\ \beta = \beta(S, \dot{S}, t) \end{cases}. \quad (17)$$

Then, the control objective is to elaborate an STA that enforces the adopted SS and its first derivative within to tend to zero in a finite time even in the presence of unknown disturbances and uncertainties with an unknown boundary. The expressions of the adopted time-varying switching gains are as follows:

$$\begin{cases} \dfrac{d}{dt}\alpha = \begin{cases} \omega_1\sqrt{\dfrac{\gamma_1}{2}}\text{sign}(\left|S\right| - \mu), & \text{if } \alpha > 0 \\ 0, & \text{if } \alpha = 0 \end{cases}, \\ \beta = 2\varepsilon\alpha \end{cases} \quad (18)$$

where ω_1, γ_1, μ, and ε are arbitrary positive constants.

Thus, for any initial condition, that is, x(0) and S(0), the proposed control law will drive the system states to an ideal 2-sliding mode in a finite time [22, 23]. To put in this time-varying control gain, an integrator operator with an external rest signal is performed by using a positive constant initial value. This procedure allows us to keep a small gain value when the state trajectory is in the immediate proximity of the desired values. Compared with the adaptive gain structure adopted in [23], the proposed structure has the advantage of deriving the adaptive gain to the selected initial value after disturbance cancellation. Otherwise, the incessant increase in switching gain may result in the occurrence of chattering or system instability. The final expression of the control signals

TABLE I
SPIM PARAMETERS

R_{sd}: 0.473 Ω	Rated power: 1.1 kW
R_{sq}: 6.274 Ω	Rated voltage: 220 V
R_r: 5.514 Ω	Rated current: 5.1 A
L_{sd}: 0.0904 H	Rated frequency: 50 Hz
L_{sq}: 0.1099 H	Number of pole pairs: 2
L_r: 0.0904 H	Rated speed: 1430 rpm
M_{srd}: 0.0817	J: 0.9 10^{-3} kg.m^2
M_{srq}: 0.0715	f : 1.2 10^{-3} N.m.s.rad^{-1}

TABLE II
ASTA PARAMETERS

Speed controller	Current controller
$C_w = 0.1$, $\omega_1 = 5$, $\gamma_1 = 1$, $\varepsilon = 1$, $\mu = 0.01$, $\rho = 0.5$	$C_w = 0.05$, $\omega_1 = 100$, $\gamma_1 = 1$, $\varepsilon = 1$, $\mu = 0.001$, $\rho = 0.5$

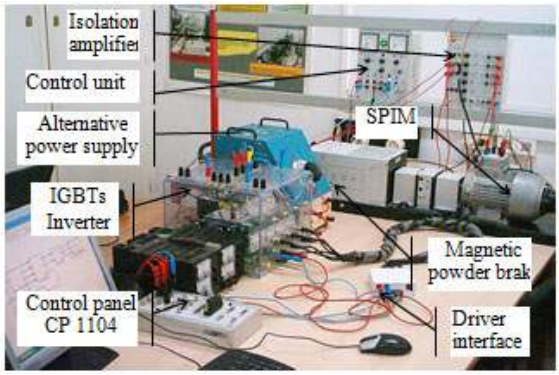

Fig. 2. Experimental setup photograph.

can be easily determined by using Equations (13), (16), and (18).

IV. Experimental Setup and Experimental Results

A. Experimental Setup Presentation

To validate the proposed ASTA, a laboratory setup is developed. A photograph of this experimental prototype is shown in Fig. 2. The experimental prototype consists of the following:

- A commercial SPIM;
- A three-leg voltage source inverter: two legs are used to drive the main and auxiliary winding voltages, and the third leg is reserved to control the offset voltage;
- A magnetic powder brake for applying the desired load torque;
- A dSPACE DS1104 controller board with a TMS320F240 slave processor and an ADC interface board CP1104;
- Three sensors for current and speed measurements are calibrated to maintain the obtained signals within the range of −10 V to 10 V, which is required by the dSPACE A/D converters.

The full implementation requires MATLAB–Simulink software that can automatically generate the C code and that can compiles, links, and downloads the control algorithm to the target digital signal processor. A sinusoidal pulse-width modulation (PWM) technique is performed to produce the PWM signals with a switching frequency of 3 kHz and a dead time of 2 μs for the three-leg inverter. Two of the PWM duty cycles are calculated according to the direct and quadratic control voltages $V_{s\alpha}^*$ and $V_{s\beta}^*$. The third duty cycle is set to 0.5 to supply a zero reference voltage. The parameters of the used SPIM are listed in Table 1, and the parameters of the speed and current controllers are detailed in Table 2.

B. Experimental Results

Three specific tests are performed wherein the reference rotor flux is kept constantly equal to the nominal value of 0.7 Wb. The experimental waveforms of the SPIM speed, d-q rotor flux, d-q currents, different SSs, and time-varying switching gain are provided.

In the first test, a nominal speed reference is applied to the SPIM followed by a sign inversion at 5 s without any load. The main aim of this test is to verify that the decoupling objective of the IRFOC strategy based on the ASTA controller is attained. The performances of the proposed control schema at a very low speed with a fixed load torque are the subject of the second test. The final test investigates the behavior of the proposed strategy under load torque variations. The experimental results obtained by using the Control Desk graphical user interface provided with dSPACE DS1104 are illustrated in the following figures.

- *Test1: SPIM experimental behavior at nominal speed consign without load torque (sign inversion)*

The first test demonstrates that the experimental rotor speed (Fig. 3) exhibits a good transient response (0.5 s) without any steady error and relevant overshoot (<3 %). Compared with the results obtained in [5] by using linear PI controllers, an improvement of approximately 50% of the time response is registered. Fig. 4 illustrates that the different SSs relative to the speed, direct and quadratic currents, are reached in a finite time. Then, the considered states are still on. The direct and quadratic rotor flux waveforms demonstrate that the rotor flux is completely aligned with the direct axis (Fig. 5). Fig. 6 proves that the decoupled objective of the IRFOC strategy is entirely achieved. The time-varying gain (Fig. 7) increases continuously when the speed tracking error is far from zero and maintains a small constant value when this error is almost equal to zero, respectively. This result is in perfect agreement with the control design objectives and results in significant chattering reduction.

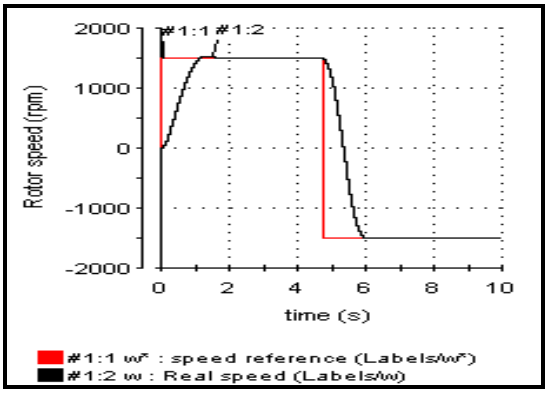

Fig. 3. Reference and experimental speed response.

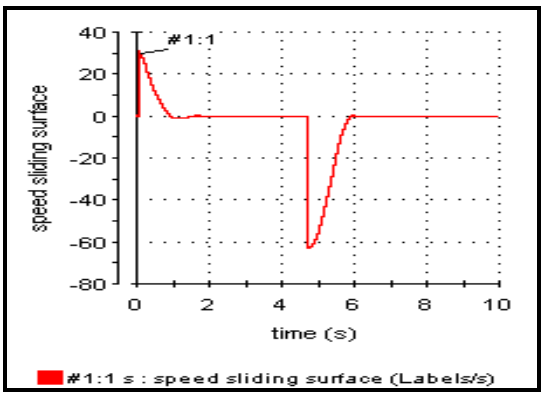

(a)

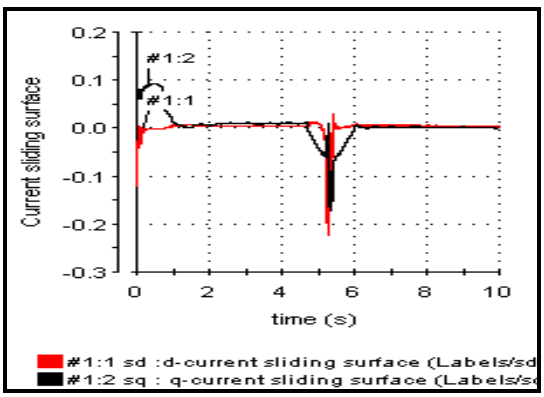

(b)

Fig. 4. (a) Speed SS. (b) Current SSs.

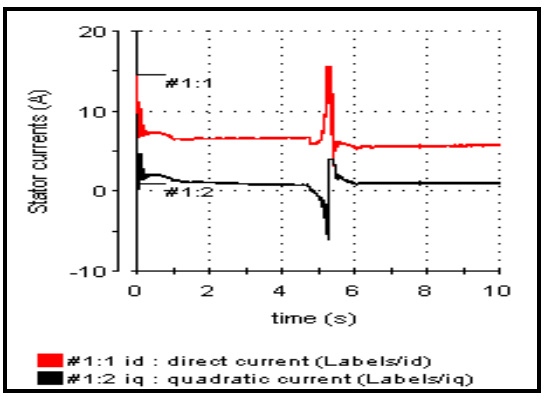

Fig. 5. Direct and quadratic experimental currents.

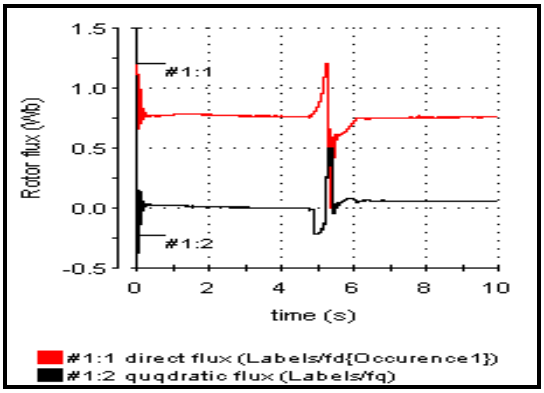

Fig. 6. Direct and quadratic experimental flux.

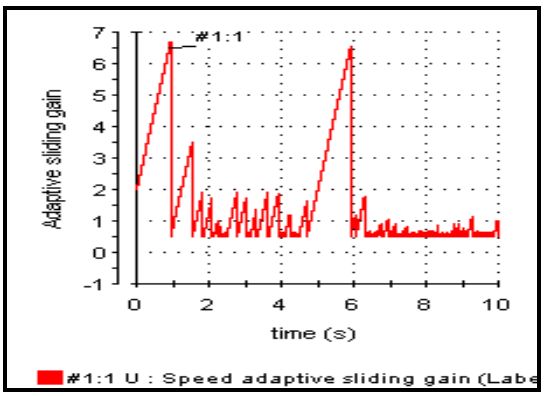

Fig. 7. Time-varying sliding gain.

- *Test 2: SPIM behavior at low speed range with load torque*

In the second test, the SPIM starts with a load torque applied via the magnetic powder brake. The response to a step speed reference of 150 rpm shows that the speed SPIM exhibits a good transient speed response even at a remarkably low speed range (Fig. 8). The direct and quadratic currents are controlled separately according to the flux and applied load torque (Fig. 10) and present insignificant oscillations. The external disturbances resulting from load torque insertion do not affect the SPIM speed response. Even during external disturbances, which are observed in the first test, the different states reach and remain in their desired SSs (Fig. 9). However, small oscillations around the desired values are registered in the speed response because of the excessive variation of the control signal by nature (Fig. 8). This result does not represent any negative effect because the variation amplitude is addressed well by the use of adaptive switching gain. The variations of time-varying gain values are shown in Fig. 11.

- *Test 3: SPIM behavior with load torque variation*

In the final test, the SPIM starts with no load. A load torque of 3 Nm is applied at 5 s, increases to 6 Nm at 10 s, and is suppressed at 15 s. Fig. 12 shows that the speed SPIM exhibits a good transient speed response and swiftly mitigates external disturbances (0.25 s). The developed electromagnetic torque

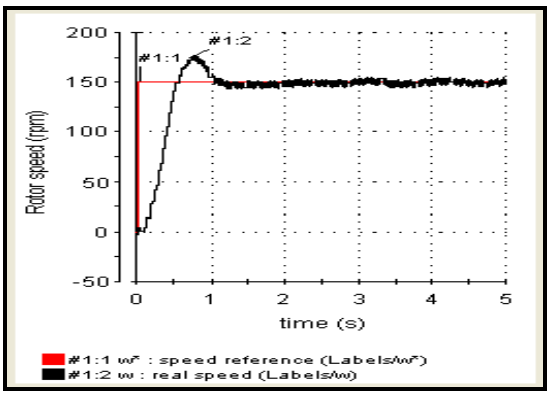

Fig. 8. Experimental speed response (low speed range).

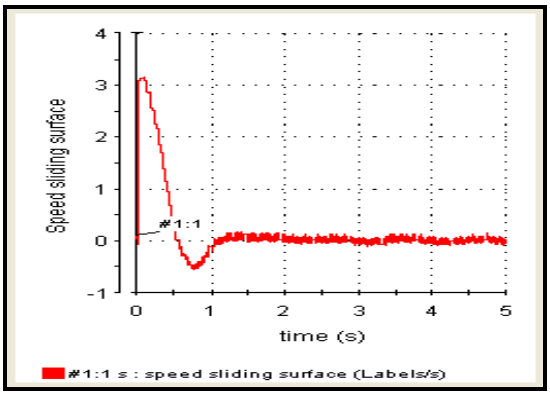

(a)

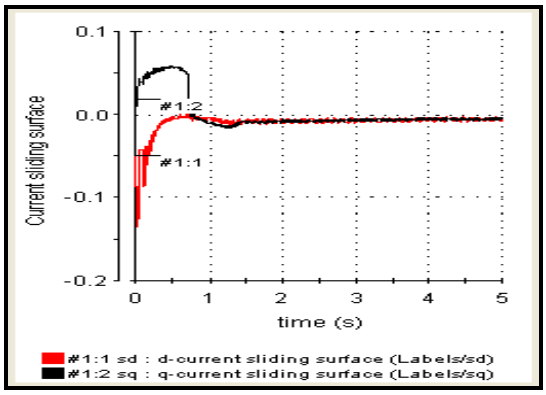

(b)

Fig. 9. (a) Speed SS. (b) Current sliding surf aces.

indicates low oscillation levels (Fig. 15). Fig. 14 illustrates the time-varying gain value that changes continuously and increases considerably when load torque is applied. After leaving the designed SS, the speed is forced to reach the designed SS again rapidly (Fig. 13). The adopted time-varying gain then delivers an adequate control signal without any need for prior knowledge of upper-limit disturbances, which is required in classical sliding mode techniques.

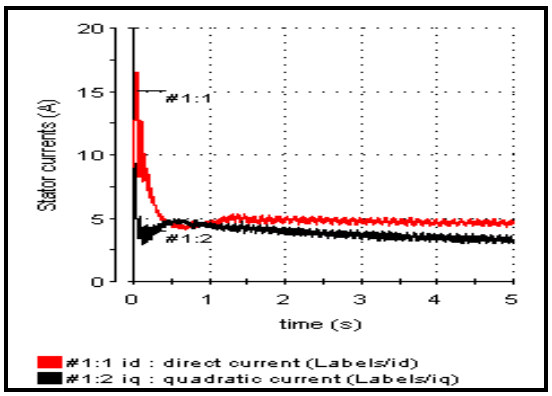

Fig. 10. Direct and quadratic experimental currents.

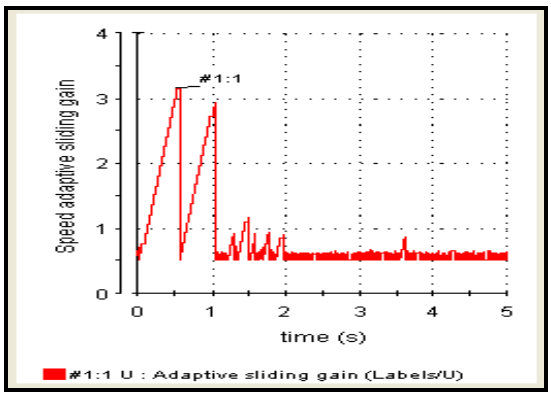

Fig. 11. Time-varying sliding gain.

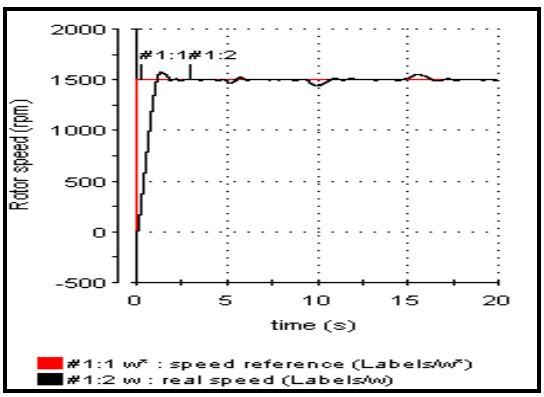

Fig. 12. Experimental speed response (load torque variation).

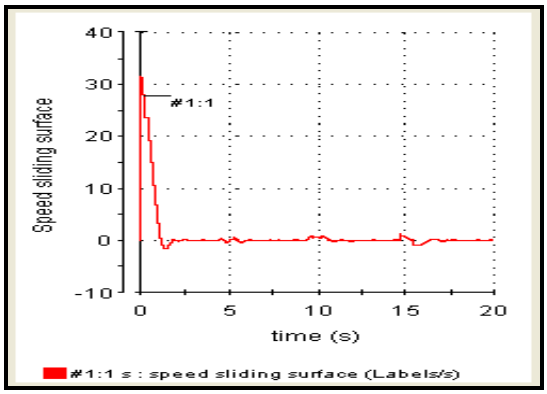

Fig. 13. *Speed SS.*

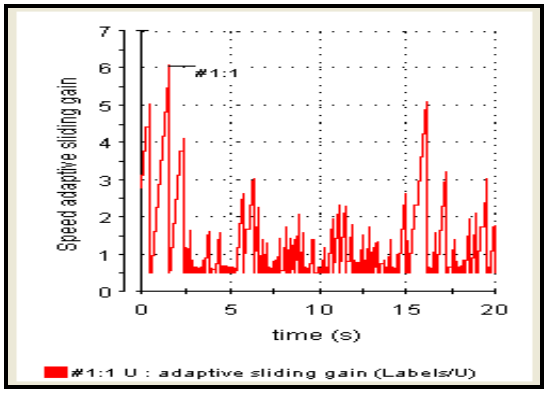

Fig. 14. Time-varying sliding gain.

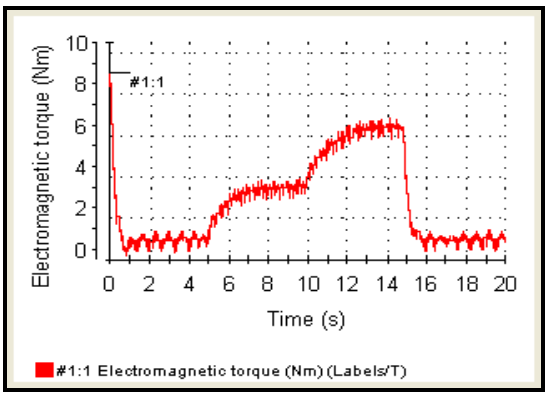

Fig. 15. Electromagnetic torque.

Therefore, the effectiveness of the proposed ASTA in terms of robustness, torque oscillation reduction, and chattering elimination has been experimentally proven even at a significantly low speed range and under unknown load conditions.

V. Conclusions

An IRFOC strategy based on a high-order sliding mode technique for controlling a SPIM has been performed and experimentally validated. A novel speed and stator currents control law has been created by using an ASTA that is associated with partial feedback linearization. The time-varying gain is calculated online according to an instantaneously SS value to avoid overestimation. The time-varying gain has been calculated without prior-knowledge of upper-limit perturbations, which are generally required in conventional sliding mode techniques. The obtained experimental results demonstrate the high performances of the designed chattering-free controllers in terms of stabilization, tracking, and robustness with respect to load conditions regarded as external disturbances even at significantly low speed ranges.

References

[1] B. Zahedi and S. Vaez-Zadeh, "Efficiency Optimization Control of Single-Phase Induction Motor Drives," *IEEE Trans. Power Electron*., Vol. 24, No. 4, pp. 1602-1070, Apr. 2009.

[2] R. Saidura, S. Mekhilef, M. B. Ali, A. Safari, and H. A. Mohammed, "Applications of variable speed drive (VSD) in electrical motors energy savings," *Renewable and Sustainable Energy Reviews*, Vol. 16, No. 1, pp. 543-550, Jan. 2012.

[3] M. Thirugnanasambandama, M. Hasanuzzaman, R. Saidur, M. B. Ali, S. Rajakarunakaran, D. Devaraj, and N. A. Rahim, "Analysis of electrical motors load factors and energy savings in an Indian cement industry," *Energy*, Vol. 36, No. 7, pp. 4307-4314, Jul. 2011.

[4] R. Saidur and TMI, Mahlia, "Impacts of energy efficiency standard on motor energy savings and emission reductions," *Clean Technology and Environmental Policy*, Vol. 13, No. 1, pp 103-109, Feb. 2011.

[5] M. Jemli, H. Ben Azza, and M. Gossa, "Real-time implementation of IRFOC for Single-Phase Induction Motor drive using dSPACE DS 1104 control board," *SMPAT*, Vol. 17, pp. 1071-1080, 2009.

[6] M. Jemli, H. Ben Azza, M. Boussak, and M. Gossa, "Sensor-less indirect stator field orientation speed control for single-phase induction motor drive," *IEEE Trans. Power Electron.*, Vol. 24, No. 6, pp. 1618-1627, Jun. 2009.

[7] M. B. R. Corrêa, C. B. Jacobina, A. M. N. Lima, and E. R. C. da Silva, "Rotor flux oriented control of a single phase induction motor drive," *IEEE Trans. Ind. Electron*., Vol. 47, No. 4, pp. 832-841, Aug. 2000.

[8] M. B. de R. Corrêa, C. B. Jacobina, E. R. Cabral da Silva, and A. M. N. Lima, "Vector control strategies for single-phase induction motor drive systems," IEEE *Trans. Ind. Electron.* Vol. 51, No. 5, pp 1073-1080, Oct. 2004.

[9] M. Guerreiro, D. Foito, and A. Cordeiro, "A speed controller for a two-winding induction motor based on diametrical inversion," *IEEE Trans. Ind. Electron.* Vol. 57, No. 1, pp. 449-456, Jan. 2010.

[10] G. J. Rubio, J. M. Cañedo, A. G. Loukianov, and J. M. Reyes, "Second order sliding mode block control of single-phase induction motors," *18th IFAC World Congress Milano*, pp. 3938-3943, Aug., 2011.

[11] G. J. Rubio, J. M. Cañedo, V. I. Utkin, and A. G. Loukianov, "Second order sliding mode block control of single-phase induction motors," *Int. J. Robust. Nonlinear Control (2012)*, Oct. 2012.

[12] Nr. Zaidi, H. Ben Azza, M. Jemli, and A. Chaari, "DSP Full implementation of second order sliding mode control to drive a SPIM," *IEEE, ICESSA,* pp. 1-6, 2013.

[13] S. C. Tan, Y. M. Lai, and Chi K. Tse, "General design issues of sliding-mode controllers in DC–DC converters," *IEEE Trans. Ind. Elect*ron., Vol. 55, No. 3, pp. 1160-1174, Mar. 2008.

[14] C. Yi Chen, "Sliding mode controller design of induction motor based on space-vector PWM method," *IJICIC*, Vol. 5, No. 10(B), pp. 3603-3614, Oct. 2009.

[15] Z. Liu and Q. Wang, "Hybrid control with sliding-mode plus self-tuning PI for electrical machines," *JEEEC*, Vol. 59, No. 3, pp. 113-121, 2008.

[16] L. Fridman and A. Levant, *Higher-Order Sliding Modes, in Sliding Mode Control in Engineering*, W. Perruquetti and J. P. Barbot, Marcel Dekker 2002.

[17] A. Levant, "Chattering analysis," *IEEE Trans. Automatic Contr*., Vol. 55, No. 6, pp. 1380-1389, Jun. 2010.
[18] M. L. Tseng and M. S. Chen, " Chattering reduction of sliding mode control by low pass filtering the control signal," *Asian Journal of Control*, Vol. 12, No. 3, pp. 392-398, May 2010.
[19] I. Boiko and L. Fridman, "Analysis of chattering in continuous sliding-mode controllers," *IEEE Trans. Automatic Contr*., Vol. 50, No. 9, pp. 1442-1446, Sep. 2005.
[20] A. Levant, "Principles of 2-sliding mode design," Science Direct, Automatica 43, pp. 576-586, 2007.
[21] A. Levant and al. "Integral high-order sliding modes," *IEEE Trans. Automatic Contr.*, Vol. 52, No. 7, pp. 1278-1282, Jul. 2007.
[22] Y. Shtessel, F. Plestan, and M. Taleb, "Lyapunov design of adaptive super-twisting controller applied to a pneumatic actuator," 18th IFAC World Congress, Milano (Italy) pp. 3051-3056, Sep, 2011.
[23] Y. B. Shtessel, J. A. Moreno, F. Plestan, L. M. Fridman, and A. S. Poznyak, "Super-twisting adaptive sliding mode control: A lyapunov design," 49th IEEE Conference on Decision and Control, Atlanta, pp.5109-5113, Dec. 2010.
[24] B. L. Cong, Z. Chen and X. D. Liu, "On adaptive sliding mode control without switching gain overestimation," Int. J. Robust. Nonlinear Control, 2012.
[25] A. F. Filippov, *Differential Equations with Discontinuous Right Handside*, Kluwer, Dordrecht, The Netherlands, 1988.
[26] M. J. Jafarian and J. Nazarzadeh, "Minimum time regulation of DC-DC converters in damping mode with an optimal adjusted sliding mode controller," *Journal of Power Electronics*, Vol. 12, No. 5, pp. 769-777, Sep. 2012.
[27] M. Dal and R. Teodorescu, "Sliding mode controller gain adaptation and chattering reduction techniques for DSP-based PM DC motor drives," *Turk J. Elec. Eng. & Comp. Sci.*, Vol. 19, No. 4, pp. 531-549, 2011.
[28] M. Caruso,V. Cecconi, A.O. Di Tommaso, and R. Rochat, "Sensorless variable speed single-phase induction motor drive system," *IEEE Inter. Conf. on Ind. Tech.* pp. 731-736, 2012.

Noureddaher Zaidi was born in Dar Belouer Sousse, Tunisia, on 2 October 1969. He received his BS and DEA degrees in electrical engineering in 1994 and 1996 from ENSET and ESSTT, University of Tunis respectively. He is currently working toward a PhD in ESSTT. His current research interests include electrical machines, sensorless vector control, AC motor drives, sliding mode control techniques.

Mohamed Jemli was born in Nasr'Allah, Tunisia, on 2 November 1960. He received his BS and DEA degrees in electrical engineering from ESSTT, University of Tunis in 1985 and 1993, respectively, and a PhD in electrical engineering from ENIT, University of Tunis in 2000. He received the HdR degree in electrical engineering in 2010 from ESSTT. He was an aggregate teacher at ISET de Radès from 1998 to 2001. He served as an assistant professor from 2001 to 2009 at ESSTT. He is currently a senior professor at ESSTT. He has authored or coauthored more than 40 papers published in international conference proceedings and technical journals. He also holds many patents. His current research interests include electrical machines, sensorless vector control of AC motor drives, advanced digital motion control, and renewable energy.

Hechmi Ben Azza was born in Bizerte, Tunisia, on 5 July 1978. He received his BS, Master, and PhD in Electrical Engineering from ESSTT, University of Tunis in 2002, 2006, and 2011, respectively. He is currently an assistant professor at ESSTT. He has published more than 14 papers in international conference proceedings and technical journals. His research interest lays in the areas of electrical machines, power conversion systems, Sensorless vector control of AC motor drives, and diagnostics.

Mohamed Boussak was born in El Haouaria, Tunisia, on 28 December 1958. He received his BS and DEA degrees in electrical engineering from ENSET, University of Tunis in 1983 and 1985, respectively; a PhD degree in electrical engineering from Pierre et Marie Curie University (Paris 6), Paris, France, in 1989; and HdR degree in electrical engineering from Aix-Marseille III University, Marseille, France, in 2004. He was a researcher from September 1989 to September 1990 and an associate professor from October 1991 to June 2004 with ESIM France. He was an associate professor of electrical machines from July 2004 to December 2008 with ECM, France. He is currently a senior professor in ECM France. His current research interests include electrical machines, power conversion systems, sensorless vector of control AC motor drives, advanced digital motion control, and diagnostics for industrial electric systems. He has authored or coauthored more than 80 papers published in scientific journals and conference proceedings. Pr. Boussak is a member of the IEEE Industry Application Society, the IEEE Industrial Electronics Society, and the IEEE Power Electronics Society. He is currently a member of the technical program committees of several international conferences and scientific journals in the field of power electronics and motor drives.